

# Liver X Receptor Modulates Diabetic Retinopathy Outcome in a Mouse Model of Streptozotocin-Induced Diabetes

Sugata Hazra,<sup>1</sup> Adil Rasheed,<sup>2</sup> Ashay Bhatwadekar,<sup>1</sup> Xiaoxin Wang,<sup>3</sup> Lynn C. Shaw,<sup>1</sup> Monika Patel,<sup>2</sup> Sergio Caballero,<sup>1</sup> Lilia Magomedova,<sup>2</sup> Nathaniel Solis,<sup>3</sup> Yuanqing Yan,<sup>1</sup> Weidong Wang,<sup>3</sup> Jeffrey S. Thinschmidt,<sup>1</sup> Amrisha Verma,<sup>4</sup> Qihong Li,<sup>4</sup> Moshe Levi,<sup>3</sup> Carolyn L. Cummins,<sup>2</sup> and Maria B. Grant<sup>1</sup>

Endothelial progenitor cells (EPCs), critical for mediating vascular repair, are dysfunctional in a hyperglycemic and/or hypercholesterolemic environment. Their dysfunction contributes to the progression of diabetic macro- and microvascular complications. Activation of “cholesterol-sensing” nuclear receptors, the liver X receptors (LXR $\alpha$ /LXR $\beta$ ), protects against atherosclerosis by transcriptional regulation of genes important in promoting cholesterol efflux and inhibiting inflammation. We hypothesized that LXR activation with a synthetic ligand would correct diabetes-induced EPC dysfunction and improve diabetic retinopathy. Studies were performed in streptozotocin (STZ)-injected DBA/2J mice fed a high-fat Western diet (DBA/STZ/WD) and treated with the LXR agonist GW3965 and in LXR $\alpha$ <sup>-/-</sup>, LXR $\beta$ <sup>-/-</sup>, and LXR $\alpha/\beta$ <sup>-/-</sup> mice. Retinas were evaluated for number of acellular capillaries and glial fibrillary acidic protein (GFAP) immunoreactivity. Bone marrow EPCs were analyzed for migratory function and gene expression. Compared with vehicle-treated DBA/STZ/WD mice, GW3965 treated mice showed fewer acellular capillaries and reduced GFAP expression. These mice also exhibited enhanced EPC migration and restoration of inflammatory and oxidative stress genes toward nondiabetic levels. LXR $\alpha$ <sup>-/-</sup>, LXR $\beta$ <sup>-/-</sup>, and LXR $\alpha/\beta$ <sup>-/-</sup> mice developed acellular capillaries and EPC dysfunction similar to the DBA/STZ/WD mice. These studies support a key role for LXR in retinal and bone marrow progenitor dysfunction associated with type 1 diabetes. LXR agonists may represent promising pharmacologic targets for correcting retinopathy and EPC dysfunction. *Diabetes* 61:3270–3279, 2012

**T**he liver X receptors (LXRs) are widely known for their important roles in modulating whole-body cholesterol homeostasis (1). LXR $\alpha$  (NR1H3) and LXR $\beta$  (NR1H2) belong to the nuclear receptor superfamily of ligand-activated transcription factors. LXR $\beta$  is ubiquitously expressed, whereas LXR $\alpha$  expression is highest in the liver, kidney, intestine, and adrenal gland. LXRs initiate a feedback response to elevated cholesterol levels by increasing the transcription of genes involved in

cholesterol catabolism and efflux when activated by their endogenous ligands (oxysterols) (2). Direct LXR target genes include the ATP-binding cassette (ABC) transporters, *ABCA1* and *ABCG1*, which govern cellular efflux of cholesterol from macrophages, as well as apolipoprotein E (*ApoE*) (1). LXR is also a key modulator of systemic inflammation (3). Because LXRs promote reverse cholesterol transport and suppress inflammatory responses, activation of LXR has been considered as a prime drug target for the treatment of the macrovascular disease atherosclerosis (4). Currently available synthetic LXR ligands (i.e., GW3965) have been shown to be effective at reducing plaque formation in animal models of atherosclerosis (5).

Inflammation and oxidative stress are central to the pathogenesis of diabetic retinopathy, a common microvascular complication of diabetes. Studies have shown inflammatory proteins are increased in the retinas or vitreous humor of diabetic animals and patients (6–8). Moreover, blocking inflammation and oxidative stress in diabetic animals prevents the development of lesions characteristic of retinopathy (9). Inflammatory molecules that have been shown to contribute to structural or functional alterations that are characteristic of retinopathy include nuclear factor (NF)- $\kappa$ B, inducible nitric oxide synthase (iNOS), cyclooxygenase (COX), intracellular adhesion molecule (ICAM), 5-lipoxygenase, interleukin (IL)-1 $\beta$ , and tumor necrosis factor (TNF)- $\alpha$  (10,11), and may represent good therapeutic targets. Likewise, the renin-angiotensin system (RAS) contains an anti-inflammatory and vascular protective axis, activated through Mas1, the putative receptor for angiotensin (Ang)-1–7, the product of ACE2 (12). Activation of this protective axis has been shown to prevent the development of diabetic retinopathy (13). To date, the effect of LXR activation on the ACE2/Ang-(1–7)/Mas1 pathway is unknown.

Although endothelial dysfunction is central to the pathogenesis of diabetic retinopathy, equally important is the lack of endothelial regeneration and repair. Bone marrow (BM)-derived endothelial progenitor cells (EPCs) are key cells responsible for maintenance and repair of the vasculature. EPCs have been shown to promote revascularization of ischemic tissues (14) and have been used for cell-based therapies to induce vascular repair, specifically for treatment of myocardial infarction (15) and peripheral arterial disease (16). EPCs function by direct incorporation into injured areas and by providing a source of growth factors and cytokines to enhance the growth potential of the resident vasculature. Cluster of differentiation (CD)34<sup>+</sup> cells are a commonly used EPC population in humans, whereas

From <sup>1</sup>Pharmacology and Therapeutics, University of Florida, Gainesville, Florida; the <sup>2</sup>Department of Pharmaceutical Sciences, University of Toronto, Toronto, Ontario, Canada; the <sup>3</sup>Department of Medicine, University of Colorado, Aurora, Colorado; and the <sup>4</sup>Department of Ophthalmology, University of Florida, Gainesville, Florida.

Corresponding author: Maria B. Grant, grantma@ufl.edu, or Carolyn L. Cummins, carolyn.cummins@utoronto.ca.

Received 16 November 2011 and accepted 30 May 2012.

DOI: 10.2337/db11-1596

S.H. and A.R. contributed equally. Senior authors M.L., C.L.C., and M.B.G. contributed equally.

© 2012 by the American Diabetes Association. Readers may use this article as long as the work is properly cited, the use is educational and not for profit, and the work is not altered. See <http://creativecommons.org/licenses/by-nc-nd/3.0/> for details.

lineage-negative (Lin<sup>-</sup>) stem-cell antigen-1 (Sca-1<sup>+</sup>) and c-Kit<sup>+</sup> double-positive cells are accepted markers for the early hematopoietic stem cell progenitors, which are the source of EPCs that give rise to endothelium and participate in vascular repair in mice (17).

EPC dysfunction has been implicated in the development of the vasodegenerative phase of diabetic retinopathy (18), and numbers of circulating EPCs are low in individuals with nonproliferative diabetic retinopathy (19). In a diabetic state, BM-derived progenitors are dysfunctional, producing fewer endothelial cells with reduced proliferative, migratory, integrative, and vasculogenic potential (20). Differentiation of BM-derived progenitor cells can be shifted away from endothelial precursors toward a proinflammatory phenotype that express a deleterious repertoire of cytokines (21).

Enhanced oxidative stress in diabetes contributes to progenitor cell dysfunction, leading to cellular and replicative senescence (22). The main components of the superoxide-generating NADPH oxidase enzyme include the membrane-associated cytochrome b558, the catalytic gp91<sup>phox</sup> (Nox2), the regulatory p22<sup>phox</sup> subunit, and cytosolic components (23). The main isoform of Nox present in BM-derived progenitors is Nox2. Increased activity of NADPH oxidase results in reduced migratory function in diabetic progenitor cells (24). Activation of the protective axis of the RAS by Ang-(1-7) via stimulation of the Mas 1 receptor results in reduced NADPH oxidase activity and improved vascular and EPC function (25).

Although there are established links between vascular disease and decreased EPCs, to date, there has been no direct association between LXR expression in EPCs and the presence of micro- or macrovascular complications. Therefore, we asked whether LXR agonists could prevent the progression of diabetic retinopathy and correct diabetes-induced EPC dysfunction in a novel accelerated model of diabetic complications, the DBA/2J mouse treated with streptozotocin (STZ) and fed a high-fat Western diet (DBA/STZ/WD).

## RESEARCH DESIGN AND METHODS

**Animals.** All animal procedures were in compliance with the National Institutes of Health (NIH) *Guide for the Care and Use of Laboratory Animals*, and with the Association for Research in Vision and Ophthalmology *Statement for the Use of Animals in Ophthalmic and Vision Research*, and were approved by the institutional animal care and use committee at the University of Colorado, the University of Toronto, and the University of Florida (UF). DBA/2J male mice were purchased from The Jackson Laboratories (Bar Harbor, ME). At 8 weeks old, mice were treated for 5 consecutive days with STZ at a concentration of 40 mg/kg body weight in 2.94% (w/v) sodium citrate (pH 4.5). Mice were fed a diet containing vehicle or the LXR agonist GW3965 (at a daily dose of 10 mg/kg) for 12 additional weeks. All DBA/2J mice were transferred to a Western (high-fat/high-cholesterol) diet (Harlan, TD 88137) for the last 4 weeks of the experiment. The Western diet was used to accelerate the progression of diabetes complications by adding hyperlipidemia to hyperglycemia, as has been previously described (26). Male wild-type (WT) and LXR $\alpha^{-/-}$ , LXR $\beta^{-/-}$ , and LXR $\alpha\beta^{-/-}$  mice on a mixed-strain background (C57BL/6:129SvEv) were maintained ad libitum on a 2916-chow diet (Harlan) in

a temperature and light-controlled environment. Experiments were performed when the animals were 5–8 months old.

**Trypsin digest and quantitation of acellular capillaries in the retina.** We examined the retinas of DBA/WD control mice and DBA/STZ/WD, untreated or treated with GW3965 ( $n = 6$  for each group), and WT, LXR $\alpha^{-/-}$ , LXR $\beta^{-/-}$ , and LXR $\alpha\beta^{-/-}$  mice ( $n = 3$  for each group) using trypsin digests as previously described (27,28).

**Assessment of inflammatory cell and activated retinal glia.** Selected eyes from control and 20-week STZ-diabetic DBA/WD animals were processed as previously described (28), and the sections were reacted with antibody to glial fibrillary acidic protein (GFAP, BD Biosciences, San Jose, CA) for detection of Müller glia, CD45 (BD Biosciences), or to CD11b (Wako Chemicals) for detection of inflammatory monocytes and ionized calcium binding adaptor molecule 1 (Iba1) (Wako Chemicals) as a marker of microglia, followed by appropriate species-specific fluorescent-conjugated secondary antibodies. Sections were examined and images were captured using epifluorescence. Numbers of positive cells were counted by observers masked to the treatment from at least three random sections per eye. Counts from multiple sections were averaged, and that value was considered as a single sample for that particular eye. Three eyes from each group were assessed in this manner.

**BM progenitor isolation and migration experiments.** The femur and tibia of each mouse were flushed, and progenitors were enriched from BM mononuclear cells with mouse hematopoietic progenitor cell enrichment kits according to the manufacturer's instruction (STEMCELL Technologies Inc., Vancouver, BC, Canada). Progenitors were tested for their migratory ability toward 100 nmol/L stromal cell-derived growth factor (SDF)-1 $\alpha$  (R&D Systems, Minneapolis, MN) with the Q<sup>CM</sup> Chemotaxis cell migration assay (Chemicon International, Inc., Temecula, CA) according to the manufacturer's instructions.

**Mouse model of oxygen-induced retinopathy (OIR).** C57BL/6J timed-pregnant mice were obtained from The Jackson Laboratories and were housed in the UF Animal Care facilities. In the neonatal mouse model of OIR, 7-day-old mice were placed with their nursing dams in a 75% oxygen atmosphere for 5 days. On postnatal day (PND) 12 and continuing through PND 17, mouse pups received twice-daily gavage (10  $\mu$ L/gavage) of vehicle (0.9% sodium chloride) or GW3965 (0.05 mg/mouse/day). On the fifth day after return to normoxia (PND17), the animals were euthanized. The eyes were processed and sections were stained with hematoxylin and eosin (H&E) and analyzed as previously described (29). The efficacy of treatment was calculated as the average percentage of nuclei per section in the eye of the GW3965-treated pups versus the eye of vehicle-treated pups. Each data point represents a minimum of one eye each from six pups.

**Retinal histology in LXR $^{-/-}$  mice.** Eyes from WT, LXR $\alpha^{-/-}$ , LXR $\beta^{-/-}$ , and LXR $\alpha\beta^{-/-}$  mice ( $n = 3$ /group) were enucleated, fixed, and sectioned for H&E staining as previously described (29). Three individuals who were masked to the identity of the H&E sections performed a pathologic examination of the slides.

**Retinal flat mounts and collagen IV staining.** Neural retinas ( $n = 3$ /group), consisting of WT, LXR $\alpha^{-/-}$ , LXR $\beta^{-/-}$ , and LXR $\alpha\beta^{-/-}$ , were processed as previously described and stained with rabbit anticollagen IV (Abcam, San Francisco, CA), followed by goat anti-rabbit IgG conjugate to DyLight 649 (Abcam) to label vasculature (18). Laser scanning confocal microscope (Leica TCS SP2, Leica Microsystems, Buffalo Grove, IL) was used, and six random fields were captured for each retina. Total numbers of junction points of each field and branch length was measured from the compressed images using ImageJ software.

**Real-time quantitative PCR.** Total RNA was extracted from mouse BM or from human CD34<sup>+</sup> EPCs and reverse transcribed as described (30). Real-time PCR was carried out using TaqMan Gene Expression Assays (Applied Biosystems, Carlsbad, CA; *h $\beta$ -actin*, *hNOX2*, *mIl-1 $\beta$* , *mNox2*, *mMas1*) or SYBR green (*mAbca1*, *mAbcg1*, *mCyclophilin*, *mIl-1 $\beta$* , *mLxra*, *mLxr $\beta$* , *mNf- $\kappa$  $\beta$* , *mNox2*), both with universal PCR Master Mix (Applied Biosystems). Primer sequences are available upon request. Relative mRNA levels were calculated using the comparative Ct method normalized to cyclophilin for mouse studies and  $\beta$ -actin for human studies.

TABLE 1  
Metabolic parameters of DBA/2J mice fed a WD

	DBA/WD + veh $n = 4$	DBA/WD + GW3965 $n = 6$	DBA/STZ/WD + veh $n = 6$	DBA/STZ/WD + GW3965 $n = 6$
Body weight (g)	35.3 $\pm$ 0.3	38.7 $\pm$ 0.7*	21.6 $\pm$ 0.7#	20 $\pm$ 1#
Plasma glucose (mg/dL)	231 $\pm$ 70	269 $\pm$ 48	727 $\pm$ 22#	820 $\pm$ 16#

\* $P < 0.05$  compared with vehicle-treated mice. # $P < 0.05$  compared with DBA/WD of the same treatment group.

**Cholesterol content.** The cholesterol content of an isolated neural retina from an individual mouse was determined by liquid chromatography tandem mass spectrometry (LC/MS/MS) after lipid extraction using a modified Folch procedure. Each sample was spiked with 0.35  $\mu\text{g}$  cholesterol- $\text{d}_7$  to normalize for extraction efficiency. Dried lipid extracts were resuspended in 100  $\mu\text{L}$  high-performance liquid chromatography-grade methanol before injection of 1  $\mu\text{L}$  to the LC/MS/MS. LC/MS/MS-run parameters used were as previously

described (31). The peak area for cholesterol was normalized to that of cholesterol- $\text{d}_7$  and then normalized to the total amount of RNA extracted to account for any differences in tissue input.

**Flow cytometry and in vitro treatment of total BM cells with GW3965.** Total BM-derived cells from WT and LXR $\alpha/\beta^{-/-}$  mice (8 months old) were stained with CD117 (c-Kit, PerCP-Cy5.5-conjugated 2B8; BD Biosciences), 0.25  $\mu\text{g}/10^6$  cells and Ly6A/E (Sca-1, PE-Cy7-conjugated D7; BD Biosciences),

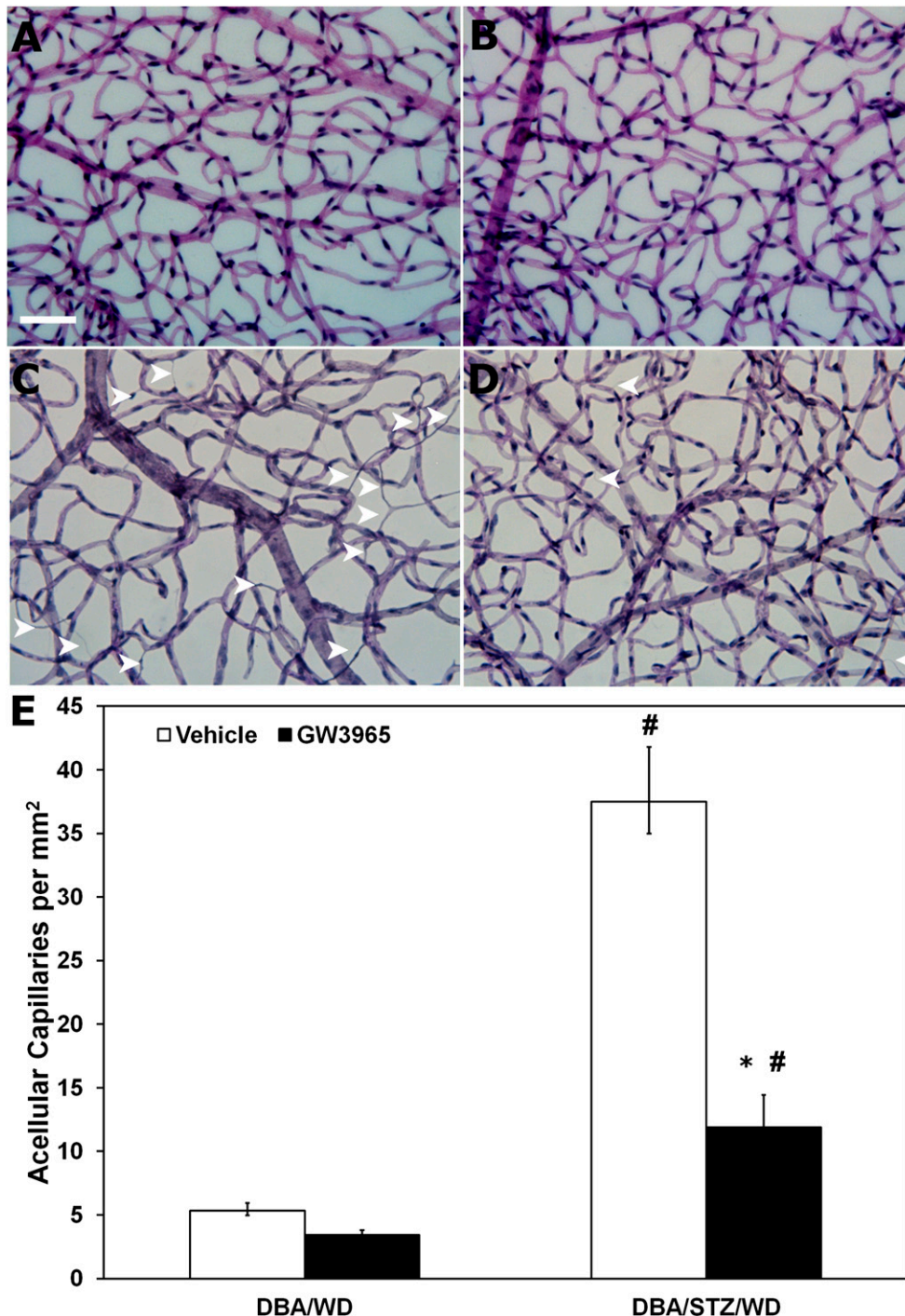


**FIG. 1.** GW3965 treatment reduces acellular capillaries in the retina of STZ-diabetic mice. *A–D*: Representative images of retinal vasculature from vehicle- (*A* and *C*) and GW3965- (*B* and *D*) treated DBA/WD (*A* and *B*) and DBA/STZ/WD mice (*C* and *D*). GW3965 was incorporated into the diet for the duration of the study. The retinas were prepared by trypsin digestion and stained with hematoxylin and periodic acid Schiff. Reduced numbers of acellular capillaries (arrowheads) were observed in retinal vasculature isolated from GW3965-treated DBA/STZ/WD (*D*) compared with vehicle-treated (*C*). *E*: Quantitative measurements of acellular capillaries. Data have been plotted as mean  $\pm$  SEM ( $n = 6$  per group). \* $P < 0.05$  compared with vehicle treated. # $P < 0.05$  compared with DBA/WD of same treatment group. (A high-quality digital representation of this figure is available in the online issue.)

1  $\mu\text{g}/10^6$  cells, followed by LIVE/DEAD Fixable Dead Cell Stain (Invitrogen), 1  $\mu\text{L}/10^6$  cells. Samples were fixed with IC Fixation Buffer (eBioscience) and stored at 4°C until analysis. Sample acquisition was performed in a FACSaria cytometer (BD Biosciences), and analysis was performed using FlowJo (Tree Star). For in vitro treatment experiments, total BM-derived cells from WT and LXR $\alpha/\beta^{-/-}$  mice (5 months old) were cultured for 48 h in culture medium (DMEM + 10% FBS + 1 $\times$  Fungizone  $\pm$  1  $\mu\text{mol/L}$  GW3965) and then collected for RNA extraction and gene expression analysis.

**CD34<sup>+</sup> EPC isolation and treatment.** CD34<sup>+</sup> cells were isolated from the peripheral blood of healthy human donors after UF institutional review board approval. The collected blood was layered on top of Ficoll (GE Healthcare, Uppsala), and mononuclear cells were enriched for CD34<sup>+</sup> using a human progenitor cell enrichment kit (STEMCELL Technologies, Inc.). Cells were suspended in media (Stem Span, STEMCELL Technologies, Inc.) with Stem Span CC100 cytokine cocktail (STEMCELL Technologies, Inc.), treated with GW3965 (0, 0.1, or 1  $\mu\text{mol/L}$ ) overnight and used for subsequent experiments.

**Statistical analysis.** A Student *t* test was used for comparisons between two groups. One-way ANOVA, followed by the Tukey post hoc test, was used for multiple comparisons. All values are expressed as mean  $\pm$  SEM. A value of  $P < 0.05$  was considered to be statistically significant. Statistical tests were performed using statistics software (SPSS Inc., Chicago, IL, or GraphPad Software, La Jolla, CA).

## RESULTS

**Chronic treatment of STZ diabetic mice with LXR agonist (GW3965) prevents the development of diabetic retinopathy and reduces inflammatory cells in the retina.** Mice of the DBA/2J strain spontaneously develop ocular abnormalities, including glaucomatous loss of retinal ganglion cells, Müller glia activation, and at 8 and

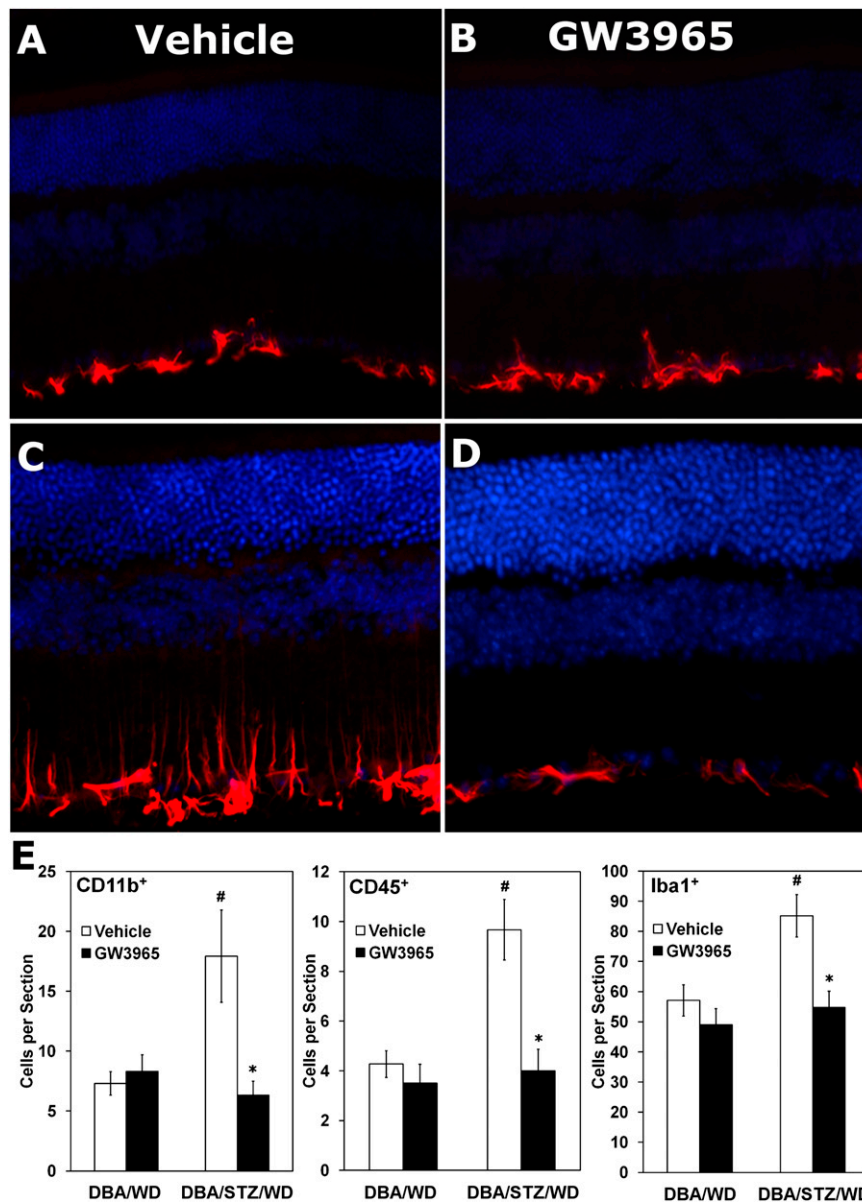


**FIG. 2.** Activated glia and inflammatory monocytes in vehicle-treated and GW3965-treated STZ-diabetic DBA/Wd mouse retinas. *A–D*: Representative images of GFAP expression in vehicle- (*A* and *C*) and GW3965- (*B* and *D*) treated DBA/Wd (*A* and *B*) and DBA/STZ/Wd (*C* and *D*) retinas. In DBA/STZ/Wd mice (12 weeks of hyperglycemia, 4 weeks of WD), GFAP expression was elevated in Müller glial cells in retinas of the vehicle-treated animals (*C*), whereas the expression was reduced in retinas from GW3965-treated animals (*D*). *E*: Quantification of CD11b<sup>+</sup>, CD45<sup>+</sup>, and Iba1<sup>+</sup> cells shows a significant increase in all three inflammatory cell types in the retinas of 20-week-old DBA/STZ/Wd mice. GW3965 returns the numbers of these inflammatory cells to control levels when DBA/STZ/Wd mice are fed the LXR agonist. Data have been plotted as mean  $\pm$  SEM ( $n = 3$  per group). \* $P < 0.05$  compared with DBA/STZ/Wd mice. # $P < 0.05$  compared with DBA/Wd of same treatment group. (A high-quality digital representation of this figure is available in the online issue.)

11 months, signs of neovascularization (32). We reasoned that in this model, the superimposition of STZ-induced diabetes and feeding of the high-fat WD would accelerate the vascular phenotype typically associated with diabetes. The metabolic characteristics of these mice are described in Table 1. Although GW3965 has been reported to improve hyperglycemia in a high-fat diet model of diabetes (5), we did not observe a change in glycemic control with our 12-week study (Table 1). Compared with control (Fig. 1A), the STZ-treated mice (Fig. 1C) showed a dramatic increase in acellular capillaries (Fig. 1E). GW3965 treatment resulted in a 50% reduction in the number of acellular capillaries ( $P < 0.05$ ) in the treated group (Fig. 1D) compared with vehicle-treated diabetic mice (Fig. 1C). Nondiabetic mice treated with GW3965 (Fig. 1B) showed no change in the number of acellular capillaries compared with the vehicle-treated nondiabetic mice (Fig. 1A).

To determine whether this change in the number of acellular capillaries was associated with reduced inflammation,

GFAP expression in Müller glial cells was assessed in retinas from vehicle- and GW3965-treated DBA/STZ/WD mice (Fig. 2). Nondiabetic DBA/WD mice (Fig. 2A) showed low levels of GFAP expression, as did the GW3965-treated nondiabetic mice (Fig. 2B). In contrast, there was a marked increase in GFAP expression in the DBA/STZ/WD mice (Fig. 2C), which was strikingly reduced in the GW3965-treated DBA/STZ/WD mice (Fig. 2D). GW3965 treatment also reduced diabetes-induced ocular inflammation to baseline levels, as assessed by a significant decrease in CD11b<sup>+</sup> cells (Fig. 2E, left panel), CD45<sup>+</sup> cells (Fig. 2E, center panel), and Iba1<sup>+</sup> microglia (Fig. 2E, right panel) in the DBA/STZ/WD mice.

**LXR agonist GW3965 enhances EPC function in STZ-diabetic mice.** One mechanism to assess the overall function of EPCs is to measure their ability to migrate toward chemoattractants. Treatment with GW3965 resulted in a significant increase ( $P < 0.05$ ) in migration of EPCs toward SDF-1 $\alpha$  (100 nmol/L) isolated from WT C57BL/6J mice (Fig. 3A, left black bar). Similarly, treatment with

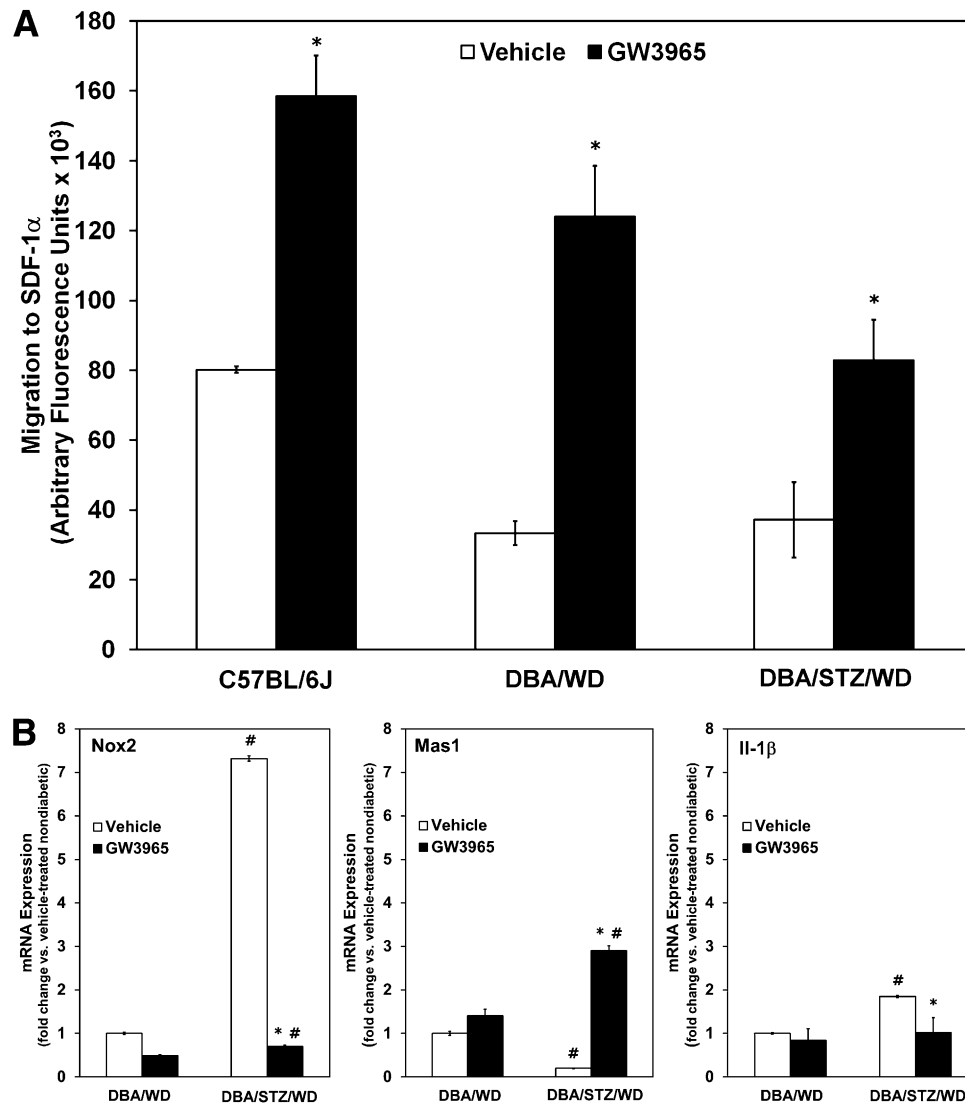


**FIG. 3.** GW3965 treatment improves the migratory response and gene expression profile of EPCs. **A:** EPCs isolated from C57BL/6J, DBA/WD, and DBA/STZ/WD mice fed a diet containing GW3965 demonstrate improved migratory response toward SDF-1 $\alpha$  compared with mice fed a vehicle-treated diet. \* $P < 0.05$  relative to vehicle control. **B:** BM-derived cells from DBA/WD and DBA/STZ/WD mice fed diets containing vehicle or GW3965 were analyzed for *Nox2*, *Mas1*, and *Il-1 $\beta$*  gene expression. The data have been normalized to the age-matched, nondiabetic vehicle-fed DBA/WD mice and plotted as mean  $\pm$  SEM ( $n = 3-4$  per group). \* $P < 0.05$  compared with respective vehicle control. # $P < 0.05$  compared with DBA/WD of same treatment group.

GW3965 resulted in an increase ( $P < 0.05$ ) in migration of the EPCs isolated from DBA/WD mice (Fig. 3A, center black bar) and DBA/STZ/WD (Fig. 3A, right black bar) compared with cells isolated from vehicle-treated mice (Fig. 3A, white bars). These data demonstrate that the improved EPC function observed after LXR activation occurs independent of the mouse model used.

To determine whether the functional differences could be accounted for by changes in expression levels of *Nox2* (Fig. 3B, left panel), *Mas1* (Fig. 3B, center panel) and *Il-1 $\beta$*  (Fig. 3B, right panel), we analyzed BM-derived cells from each of the DBA/2J treatment groups described above (Fig. 3). Quantitative PCR analysis demonstrated a significant increase in the expression of *Il-1 $\beta$*  in DBA/STZ/WD mice compared with DBA/WD mice. This increase in STZ-injected mice was significantly attenuated in the diabetic mice treated with GW3965 (Fig. 3B). Likewise, treatment with GW3965 in DBA/STZ/WD mice resulted in a 10-fold reduction in *Nox2*, the main isoform of Nox expressed in BM cells that is responsible for superoxide generation, while increasing the mRNA expression of the protective *Mas1* receptor (Fig. 3B), supporting a direct association between LXR activation and the protective axis of the RAS.

#### Supplementation with GW3965 results in a reduction of preretinal neovascularization in the OIR model.

Rodent models of STZ diabetes do not develop retinal angiogenesis, as is characteristic of advanced human disease. Therefore, we used a well-established model of retinal angiogenesis in mice, the OIR model. In this model, nursing dams and their pups were placed at 75% oxygen on PND 7. The high oxygen level interrupts normal retinal blood vessel development. On PND 12, the mice were returned to normal room air (21% oxygen). On PND 17, the pups were killed and cross-sections of the retinas showed that preretinal blood vessels, a measure of the level of retinopathy, were markedly reduced in pups treated with GW3965 ( $62 \pm 10$  vs.  $88 \pm 8$  [vehicle] preretinal nuclei/retinal cross-sections). This represented a nearly 30% reduction in preretinal neovascularization ( $P < 0.05$ ; Fig. 4).

**LXR $\alpha/\beta^{-/-}$  mice have a greater number of acellular capillaries and reduced numbers of reparative EPCs with decreased migratory capacity.** Consistent with the role of LXRs in modulating cholesterol content, we found the cholesterol content of the neural retina was increased in the LXR $\alpha/\beta^{-/-}$  mice compared with WT ( $P = 0.05$ ; Fig. 5A). Previous studies have shown that LXR $\alpha/\beta^{-/-}$  mice have elevated intracellular cholesterol levels in numerous tissues, including the liver, adrenal gland, and macrophages (33–35). However, cholesterol and triglyceride levels in the serum are lower in the LXR $\alpha/\beta^{-/-}$  mice compared with WT mice (36), and the LXR $\alpha/\beta^{-/-}$  mice are normoglycemic and tend to be more insulin-sensitive compared with WT mice (30). In LXR $\alpha/\beta^{-/-}$  mice, cholesterol can accumulate in tissues because there is an impaired capacity to efflux the cholesterol back into circulation. We measured the gene expression of two cholesterol transporters important in cholesterol efflux (*Abca1* and *Abcg1*) using quantitative PCR. *Abca1* and *Abcg1* were both strongly repressed in the neural retinas from LXR $\alpha/\beta^{-/-}$  mice ( $P < 0.05$ ; Fig. 5B). There were no significant differences in the levels of the inflammatory markers *Il-1 $\beta$*  and *Nf- $\kappa$ B* in the retinas of LXR $\alpha/\beta^{-/-}$  compared with WT mice (data not shown). However, the expression of *Nox2* was increased in the LXR $\alpha/\beta^{-/-}$  mice ( $P = 0.05$ ; Fig. 5B), suggesting that increased reactive oxygen species may be present in the retinas of these mice.

Our gain of function studies using the LXR agonist clearly demonstrated protection from the development of retinopathy; thus, we reasoned that the loss of LXR activation in the retina may lead to pathology. This was confirmed, because LXR $\alpha^{-/-}$ , LXR $\beta^{-/-}$ , and LXR $\alpha/\beta^{-/-}$  mice exhibited increased numbers of acellular capillaries compared with the WT mice (Fig. 5C and D). To exclude the possibility that the LXR knockout mice had intrinsic abnormalities in their retinas, we performed H&E staining of retinal cross-sections of WT, LXR $\alpha^{-/-}$ , LXR $\beta^{-/-}$  and LXR $\alpha/\beta^{-/-}$  mice. We did not observe any difference in retinal thickness or morphology between the experimental groups (data not shown). We also performed retinal flat mounts to examine the integrity and pattern of the retinal vasculature. No differences were detected in the vasculature between groups of mice, as assessed by numbers of junctions and branch lengths (data not shown).

We next assessed whether the LXR $\alpha/\beta^{-/-}$  mice would have a defect in their EPCs that could be contributing to the development of retinopathy. LXR $\alpha/\beta^{-/-}$  mice had reduced numbers of Sca-1<sup>+</sup>/c-Kit<sup>+</sup> progenitor cells within their BM compared with WT mice (Fig. 6A). Furthermore, Lin<sup>-</sup> Sca-1<sup>+</sup> progenitor cells isolated from LXR $\alpha/\beta^{-/-}$  mice exhibited significantly reduced migration to SDF-1 $\alpha$  compared with Lin<sup>-</sup> Sca-1<sup>+</sup> cells isolated from WT mice (Fig. 6B). Gene expression analyses from total BM of WT versus LXR $\alpha/\beta^{-/-}$  mice demonstrated that LXR $\alpha/\beta^{-/-}$  cells had significantly reduced *Lxra* and *Lxrb* mRNA, as expected, while having increased levels of *Nf- $\kappa$ B* and *Il-1 $\beta$* , and *Nox2* mRNA (Fig. 6C). Furthermore, in vitro LXR agonist treatment of BM-derived cells from WT and LXR $\alpha/\beta^{-/-}$  mice showed repression of both *Nf- $\kappa$ B* and *Nox2* in the WT mice, while having no effect in the LXR $\alpha/\beta^{-/-}$  mice, as expected (Fig. 6D). No significant change was observed with *Il-1 $\beta$*  in any of the groups (data not shown).

**LXR agonist reduces a key marker of oxidative stress in human CD34<sup>+</sup> EPCs.** Human CD34<sup>+</sup> EPCs isolated from healthy donors and treated ex vivo with the LXR agonist GW3965 (0, 0.1, or 1  $\mu$ mol/L) showed a marked

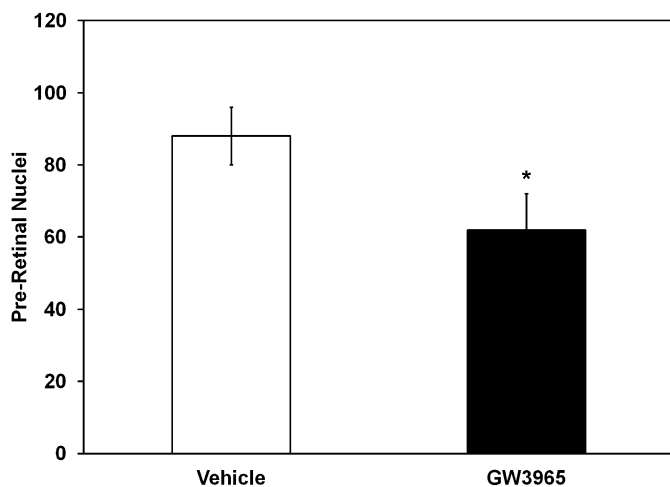
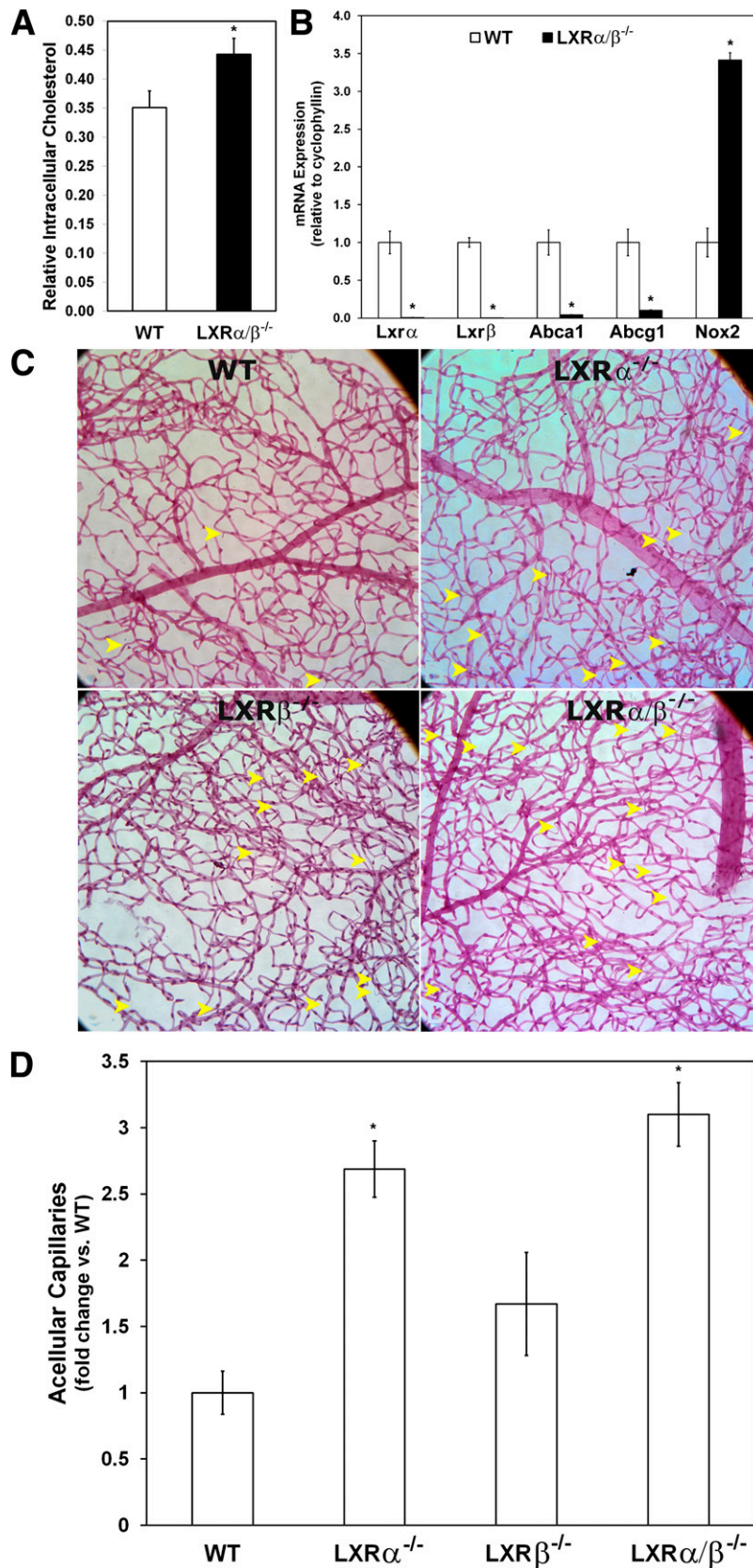
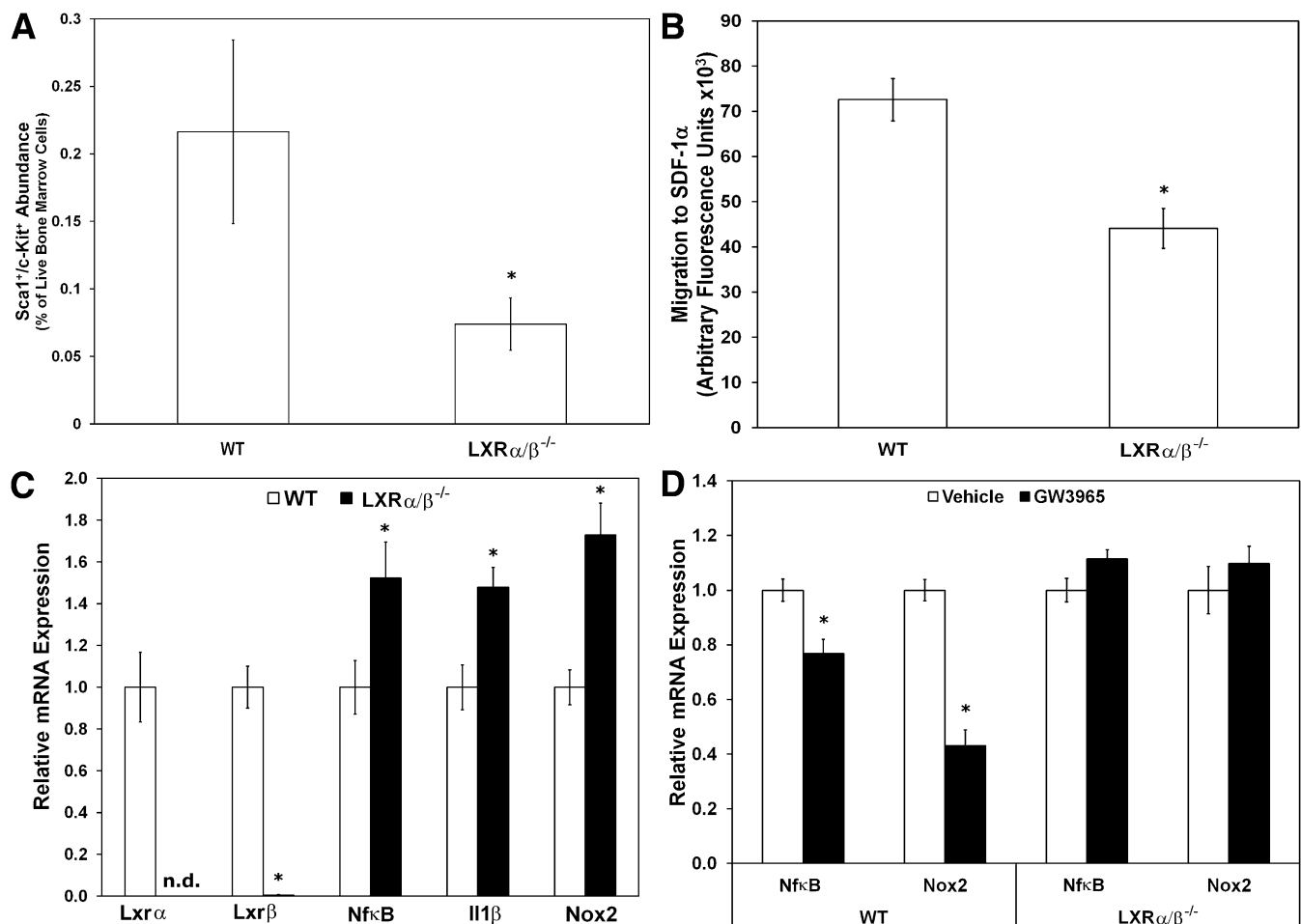


FIG. 4. GW3965 treatment reduces preretinal neovascularization in the OIR model. Mouse pups treated with GW3965 have a significant reduction in preretinal neovascularization compared with vehicle treatment. Data have been plotted as mean  $\pm$  SEM ( $n = 6$  per group). \* $P < 0.05$  compared with vehicle treatment.



**FIG. 5.** Loss of LXR leads to retinal vascular injury and formation of acellular capillaries. **A:** Cholesterol content for neural retinal cells is increased in LXR $\alpha/\beta^{-/-}$  mice compared with WT mice. Relative cholesterol levels measured by LC/MS/MS are calculated after normalizing for the extraction efficiency of an internal standard (cholesterol- $d_7$ ) and for the RNA content of the extracted tissue ( $n = 4-6$  per group). **B:** Gene expression analysis of neural retinas derived from WT and LXR $\alpha/\beta^{-/-}$  mice and normalized to the WT group for each gene ( $n = 3-6$  per group). **C:** Representative images of retinal vasculature from WT, LXR $\alpha^{-/-}$ , LXR $\beta^{-/-}$ , and LXR $\alpha/\beta^{-/-}$  mice. Acellular capillaries are indicated with *arrowheads*. Increased numbers of acellular capillaries were observed in retinal vasculature isolated from LXR knockout mice compared with WT, with the greatest degree of acellularity shown by the LXR $\alpha/\beta^{-/-}$  mice. **D:** Quantitative measurements of acellular capillaries ( $n = 3$  per group). Data have been plotted as mean  $\pm$  SEM. \* $P < 0.05$  compared with WT. (A high-quality digital representation of this figure is available in the online issue.)



**FIG. 6.** Characterization of number, function, and gene expression of cells isolated from  $LXR\alpha/\beta^{-/-}$  mice.  $LXR\alpha/\beta^{-/-}$  mice showed reduced number of Sca-1<sup>+</sup>/c-Kit<sup>+</sup> cells in BM as measured by flow cytometry ( $n = 8-10$  per group) (A), reduced migratory response of EPCs isolated from BM to SDF-1 $\alpha$  (B), and increased expression of inflammatory markers *Nf- $\kappa$ B* and *Il-1 $\beta$*  and the oxidative stress marker *Nox2* in BM-derived cells from  $LXR\alpha/\beta^{-/-}$  mice ( $n = 7-9$  per group) (C) compared with WT. D: Gene expression analysis of BM-derived cells from WT and  $LXR\alpha/\beta^{-/-}$  mice cultured in vitro for 48 h with vehicle or 1  $\mu$ mol/L GW3965 ( $n = 5-9$  per group). Gene expression data have been normalized to the WT or vehicle group for each gene and plotted as mean  $\pm$  SEM. \* $P < 0.05$  compared with WT (A, B, C). \* $P < 0.05$  compared with vehicle treatment (D).

reduction of *NOX2* mRNA expression (Fig. 7), similar to that seen in DBA/STZ/WD mouse BM-derived cells treated with GW3965 (Fig. 3B).

## DISCUSSION

Although there are established links between vascular disease and decreased EPC number and function, this is the first study to examine the association between LXR expression in EPCs and the presence of retinopathy. DBA/STZ/WD mice treated with the LXR agonist GW3965 showed fewer acellular capillaries and reduced GFAP expression in the retina. BM-derived progenitor cells from DBA/STZ/WD mice treated with GW3965 showed improved migratory function compared with cells isolated from vehicle-treated DBA/STZ/WD mice. Although we observed a protective effect of LXR activation, the absence of  $LXR\alpha/\beta^{-/-}$  resulted in phenotypic vascular changes similar to those observed in diabetes despite the lack of metabolic dysfunction.  $LXR\alpha/\beta^{-/-}$  mice showed increased acellular capillaries in the retina along with fewer Sca-1<sup>+</sup>/c-Kit<sup>+</sup> cells in their BM; furthermore, Lin<sup>-</sup>/Sca-1<sup>+</sup> cells from  $LXR\alpha/\beta^{-/-}$  mice exhibited decreased migratory capacity compared

with those from WT mice. *Nox2*, the catalytic subunit of NADPH oxidase, was increased in BM-derived cells of DBA/STZ/WD origin, and treatment with the LXR agonist, GW3965, resulted in a dramatic reduction in *Nox2* mRNA expression (Fig. 3B). Importantly, activation of LXR using GW3965 in human CD34<sup>+</sup> cells similarly resulted in downregulation of *NOX2* mRNA (Fig. 7). Thus, LXR activation would serve to reduce oxidative damage, and these results suggest that LXR agonists may represent promising pharmacologic targets for correcting diabetes-induced retinopathy and EPC dysfunction.

There is increasing evidence for a link between cholesterol levels and EPC function (37,38). Hypercholesterolemic patients, free of diabetes, have been found to have a reduced number of circulating EPCs with impaired function (39,40). A dose-dependent decrease in EPC survival and function was observed with exposure to oxidized LDL, and numerous in vitro and in vivo studies demonstrated that hydroxymethylglutaryl-CoA reductase inhibitors (statins) potently enhance EPC numbers and function (41-43). Hypercholesterolemia has also been linked to monocytosis in atherosclerosis (44). Animal studies have shown that increased monocytosis in response to granulocyte-macrophage

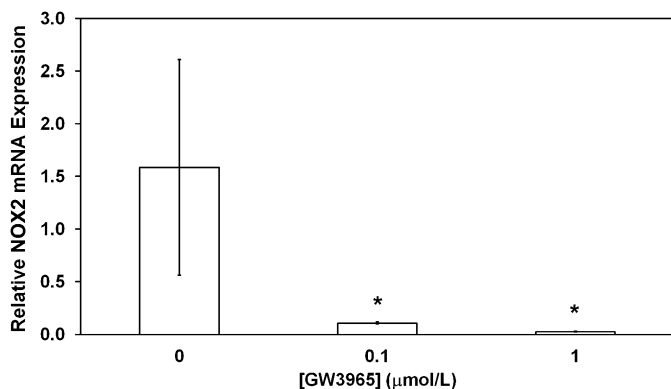


**FIG. 7. Human EPCs respond to GW3965 similar to mouse EPCs.** Human peripheral blood CD34<sup>+</sup> cells obtained from healthy donors and treated ex vivo with GW3965 show a significant decrease in *NOX2* mRNA expression compared with cells exposed to vehicle alone. Data have been plotted as mean  $\pm$  SEM ( $n = 3$  donors per group). \* $P < 0.05$  compared with vehicle treatment.

colony-stimulating factor is dependent on cellular cholesterol levels in BM-derived cells and the expression of the LXR target genes ABCA1, ABCG1, and ApoE (44).

LXR's dual role in inhibiting inflammatory cytokine expression and increasing cholesterol efflux, together with the connection between EPCs and cholesterol, lead us to hypothesize that LXR is an important determinant of EPC function. From our studies, we can conclude that both mechanisms are likely involved in delaying the progression of retinopathy. As expected, we saw increased accumulation of cholesterol in the neural retinas of LXR $\alpha/\beta$ <sup>-/-</sup> mice and strong evidence for suppression of inflammation in retinas from LXR agonist-treated DBA/STZ/WD mice. The LXR $\alpha/\beta$ <sup>-/-</sup> mice are neither hyperglycemic nor hypercholesterolemic and were not fed a high-cholesterol diet; yet, they exhibited key features of diabetic retinopathy. It is possible that the migratory defect in their EPCs may be related to the intracellular levels of cholesterol, which are known to be elevated in many tissues from LXR $\alpha/\beta$ <sup>-/-</sup> mice. Additional studies are required to specifically explore the relationship between increased circulating cholesterol, EPC function, and LXRs in the absence of diabetes. We cannot rule out the possibility that LXR activation occurs directly in the retina because high expression of LXR $\beta$  has been shown in freshly isolated and cultured retinal pigment epithelial cells (45).

The model (DBA/STZ/WD mice) used in this study has some limitations in that we superimpose STZ-induced diabetes onto the DBA/2J background, which has preexisting glaucomatous retinal pathology. However, we find that DBA/STZ/WD mice develop a similar phenotype to STZ-treated C57BL/6 mice but with an accelerated development of acellular capillaries. This is not entirely unexpected because another model of glaucoma, the retinal ischemia-reperfusion injury model, also develops acellular capillaries (46).

Development of acellular capillaries is partly due to inadequate vascular repair by EPCs. We previously showed that diabetic EPC dysfunction is due to reduced endothelial NOS expression, decreased NO bioavailability, and reduced migration in response to SDF-1 $\alpha$  (47,48). Ex vivo NADPH oxidase inhibition in diabetic cells restored migratory function in vitro and enhanced their homing to ischemic retinal vasculature in vivo. The NADPH oxidase system is a key target for correcting vasoreparative

dysfunction in diabetic EPCs. Interestingly, our current study shows that the LXR agonist GW3965 significantly decreases the expression of *Nox2*, the critical subunit in NADPH oxidase, in both murine and human progenitors. Thus, one of the major mechanisms for the beneficial effects of LXR activation in EPCs may be by reducing superoxide levels.

The vasoprotective axis (ACE2/Ang-(1-7)/Mas1) of RAS counteracts the traditional proliferative, fibrotic, proinflammatory, and hypertrophic effects of the ACE/Ang II/AT1R axis of the RAS. The importance of the vasodeleterious axis of the RAS (ACE/Ang II/AT1R) in cardiovascular disease, as well as in diabetes and diabetes complications, is well established, because ACE inhibitors and angiotensin receptor blockers are leading therapeutic strategies (49). The concept that shifting the balance of the RAS toward the vasodilatory axis by activation of ACE2 or its product, Ang-(1-7) is beneficial has been supported by many studies in cardiac, pulmonary, and vascular fibrosis (50). Our studies show that LXR agonist treatment would serve to augment this protective axis of RAS by enhancing *Mas1* expression.

In summary, our results using pharmacologic activation of LXR and genetic models deficient in LXR $\alpha$  or LXR $\beta$ , or both, suggest a novel role of LXR activation to prevent diabetic vascular pathology by downregulation of retinal inflammation and oxidative stress and activation of the protective arm of RAS. LXR activation decreased GFAP and Iba1 expression, reduced infiltration of CD11b<sup>+</sup> cells and CD45<sup>+</sup> cells within the retina, and reduced *Nox2* expression in human and murine progenitor cell studies. The activation of LXR results in enhancement of the EPC reparative function in STZ mice, as indicated by increased EPC migration and decreased expression of inflammatory and oxidative stress genes. The loss of LXR in these cells attenuates migration, even in the absence of diabetes, and results in an increase in the inflammatory (*Nf- $\kappa$ B* and *IL-1 $\beta$* ) and oxidative stress (*Nox2*) genes, similar to what are observed in progenitors from diabetic mice. Our studies strongly support the potential therapeutic utility of an LXR agonist for the treatment of diabetic retinopathy and accompanying EPC dysfunction.

#### ACKNOWLEDGMENTS

This work was supported by NIH grants EY-007739, EY-012601, U01 HL-087366, and DK-090730 to M.B.G.; NIH grants U01 DK-076134 and R01 AG-026529 to M.L.; the Kidney Foundation of Canada, the Banting and Best Diabetes Center to C.L.C.; and the Canadian Institutes of Health Research to C.L.C. and M.P. No potential conflicts of interest relevant to this article were reported.

S.H., A.R., and J.S.T. carried out research and contributed to writing the manuscript; A.B., X.W., M.P., L.M., N.S., Y.Y., W.W., A.V., and Q.L. carried out research; L.C.S. and S.C. contributed to writing the manuscript; M.L. designed research; and C.L.C. and M.B.G. designed research and contributed to writing the manuscript. M.B.G., M.L., and C.L.C. are the guarantors of this work and, as such, had full access to all of the data in the study and take responsibility for the integrity of the data and the accuracy of the data analysis.

The authors are grateful to David Mangelsdorf (University of Texas Southwestern Medical Center) for the LXR knockout mice. The authors thank Dr. Michael E. Boulton and Dr. Xiaoping Qi (UF) for their analysis of LXR knockout mice

retinal histology. The authors thank Dionne White and Natalie Simard (University of Toronto Flow Cytometry Facility), and Ranya Krishnan, Ricky Tsai, and Mitchell Han (University of Toronto), for assistance with sample collection.

## REFERENCES

- Calkin AC, Tontonoz P. Liver x receptor signaling pathways and atherosclerosis. *Arterioscler Thromb Vasc Biol* 2010;30:1513–1518
- Janowski BA, Willy PJ, Devi TR, Falck JR, Mangelsdorf DJ. An oxysterol signalling pathway mediated by the nuclear receptor LXR alpha. *Nature* 1996;383:728–731
- Zelcer N, Tontonoz P. Liver X receptors as integrators of metabolic and inflammatory signaling. *J Clin Invest* 2006;116:607–614
- Faulds MH, Zhao C, Dahlman-Wright K. Molecular biology and functional genomics of liver X receptors (LXR) in relationship to metabolic diseases. *Curr Opin Pharmacol* 2010;10:692–697
- Joseph SB, McKilligin E, Pei L, et al. Synthetic LXR ligand inhibits the development of atherosclerosis in mice. *Proc Natl Acad Sci USA* 2002;99:7604–7609
- Zhang W, Liu H, Al-Shabraway M, Caldwell RW, Caldwell RB. Inflammation and diabetic retinal microvascular complications. *J Cardiovasc Dis Res* 2011;2:96–103
- Brucklacher RM, Patel KM, VanGuilder HD, et al. Whole genome assessment of the retinal response to diabetes reveals a progressive neurovascular inflammatory response. *BMC Med Genomics* 2008;1:26
- Kern TS. Contributions of inflammatory processes to the development of the early stages of diabetic retinopathy. *Exp Diabetes Res* 2007;2007:95103
- Kowluru RA, Kanwar M, Chan PS, Zhang JP. Inhibition of retinopathy and retinal metabolic abnormalities in diabetic rats with AREDS-based micronutrients. *Arch Ophthalmol* 2008;126:1266–1272
- Zheng L, Howell SJ, Hatala DA, Huang K, Kern TS. Salicylate-based anti-inflammatory drugs inhibit the early lesion of diabetic retinopathy. *Diabetes* 2007;56:337–345
- Vincent JA, Mohr S. Inhibition of caspase-1/interleukin-1beta signaling prevents degeneration of retinal capillaries in diabetes and galactosemia. *Diabetes* 2007;56:224–230
- Ferreira AJ, Shenoy V, Qi Y, et al. Angiotensin-converting enzyme 2 activation protects against hypertension-induced cardiac fibrosis involving extracellular signal-regulated kinases. *Exp Physiol* 2011;96:287–294
- Verma A, Shan Z, Lei B, et al. ACE2 and Ang-(1–7) confer protection against development of diabetic retinopathy. *Mol Ther* 2012;20:28–36
- Urbich C, Dimmeler S. Endothelial progenitor cells: characterization and role in vascular biology. *Circ Res* 2004;95:343–353
- Sekiguchi H, Li M, Losordo DW. The relative potency and safety of endothelial progenitor cells and unselected mononuclear cells for recovery from myocardial infarction and ischemia. *J Cell Physiol* 2009;219:235–242
- Asahara T, Kawamoto A, Masuda H. Concise review: circulating endothelial progenitor cells for vascular medicine. *Stem Cells* 2011;29:1650–1655
- Grant MB, May WS, Caballero S, et al. Adult hematopoietic stem cells provide functional hemangioblast activity during retinal neovascularization. *Nat Med* 2002;8:607–612
- Caballero S, Sengupta N, Afzal A, et al. Ischemic vascular damage can be repaired by healthy, but not diabetic, endothelial progenitor cells. *Diabetes* 2007;56:960–967
- Egan CG, Lavery R, Caporali F, et al. Generalised reduction of putative endothelial progenitors and CXCR4-positive peripheral blood cells in type 2 diabetes. *Diabetologia* 2008;51:1296–1305
- Loomans CJ, de Koning EJ, Staal FJ, et al. Endothelial progenitor cell dysfunction: a novel concept in the pathogenesis of vascular complications of type 1 diabetes. *Diabetes* 2004;53:195–199
- Loomans CJ, van Haperen R, Duijs JM, et al. Differentiation of bone marrow-derived endothelial progenitor cells is shifted into a proinflammatory phenotype by hyperglycemia. *Mol Med* 2009;15:152–159
- Erusalimsky JD. Vascular endothelial senescence: from mechanisms to pathophysiology. *J Appl Physiol* 2009;106:326–332
- Frey RS, Ushio-Fukai M, Malik AB. NADPH oxidase-dependent signaling in endothelial cells: role in physiology and pathophysiology. *Antioxid Redox Signal* 2009;11:791–810
- Jarajapu YP, Caballero S, Verma A, et al. Blockade of NADPH oxidase restores vasoreparative function in diabetic CD34+ cells. *Invest Ophthalmol Vis Sci* 2011;52:5093–5104
- Sampaio WO, Souza dos Santos RA, Faria-Silva R, da Mata Machado LT, Schiffrin EL, Touyz RM. Angiotensin-(1–7) through receptor Mas mediates endothelial nitric oxide synthase activation via Akt-dependent pathways. *Hypertension* 2007;49:185–192
- Wang XX, Jiang T, Shen Y, et al. Diabetic nephropathy is accelerated by farnesoid X receptor deficiency and inhibited by farnesoid X receptor activation in a type 1 diabetes model. *Diabetes* 2010;59:2916–2927
- Bhatwadekar A, Glenn JV, Figarola JL, et al. A new advanced glycation inhibitor, LR-90, prevents experimental diabetic retinopathy in rats. *Br J Ophthalmol* 2008;92:545–547
- Li Q, Verma A, Han PY, et al. Diabetic eNOS-knockout mice develop accelerated retinopathy. *Invest Ophthalmol Vis Sci* 2010;51:5240–5246
- Pan H, Nguyen NQ, Yoshida H, et al. Molecular targeting of antiangiogenic factor 16K hPRL inhibits oxygen-induced retinopathy in mice. *Invest Ophthalmol Vis Sci* 2004;45:2413–2419
- Patel R, Patel M, Tsai R, et al. LXRβ is required for glucocorticoid-induced hyperglycemia and hepatosteatosis in mice. *J Clin Invest* 2011;121:431–441
- Wollam J, Magomedova L, Magner DB, et al. The Rieske oxygenase DAF-36 functions as a cholesterol 7-desaturase in steroidogenic pathways governing longevity. *Aging Cell* 2011;10:879–884
- Schuettauf F, Rejzda R, Walski M, et al. Retinal neurodegeneration in the DBA/2J mouse—a model for ocular hypertension. *Acta Neuropathol* 2004;107:352–358
- Bradley MN, Hong C, Chen M, et al. Ligand activation of LXR beta reverses atherosclerosis and cellular cholesterol overload in mice lacking LXR alpha and apoE. *J Clin Invest* 2007;117:2337–2346
- Cummins CL, Volle DH, Zhang Y, et al. Liver X receptors regulate adrenal cholesterol balance. *J Clin Invest* 2006;116:1902–1912
- Peet DJ, Turley SD, Ma W, et al. Cholesterol and bile acid metabolism are impaired in mice lacking the nuclear oxysterol receptor LXR alpha. *Cell* 1998;93:693–704
- Kalaany NY, Gauthier KC, Zavacki AM, et al. LXRs regulate the balance between fat storage and oxidation. *Cell Metab* 2005;1:231–244
- Croce G, Passacuale G, Necozone S, Ferri C, Desideri G. Non-pharmacological treatment of hypercholesterolemia increases circulating endothelial progenitor cell population in adults. *Arterioscler Thromb Vasc Biol* 2006;26:e38–e39
- Pirro M, Bagaglia F, Paoletti L, Razzi R, Mannarino MR. Hypercholesterolemia-associated endothelial progenitor cell dysfunction. *Ther Adv Cardiovasc Dis* 2008;2:329–339
- Chen JZ, Zhang FR, Tao QM, Wang XX, Zhu JH. Number and activity of endothelial progenitor cells from peripheral blood in patients with hypercholesterolemia [retracted in: *Clin Sci (Lond)* 2010;119:545]. *Clin Sci (Lond)* 2004;107:273–280
- Vasa M, Fichtlscherer S, Aicher A, et al. Number and migratory activity of circulating endothelial progenitor cells inversely correlate with risk factors for coronary artery disease. *Circ Res* 2001;89:E1–E7
- Fadini GP, Albiero M, Boscaro E, et al. Rosuvastatin stimulates clonogenic potential and anti-inflammatory properties of endothelial progenitor cells. *Cell Biol Int* 2010;34:709–715
- Imanishi T, Hano T, Sawamura T, Nishio I. Oxidized low-density lipoprotein induces endothelial progenitor cell senescence, leading to cellular dysfunction. *Clin Exp Pharmacol Physiol* 2004;31:407–413
- Lievadot J, Murasawa S, Kureishi Y, et al. HMG-CoA reductase inhibitor mobilizes bone marrow-derived endothelial progenitor cells. *J Clin Invest* 2001;108:399–405
- Murphy AJ, Akhtari M, Tolani S, et al. ApoE regulates hematopoietic stem cell proliferation, monocytosis, and monocyte accumulation in atherosclerotic lesions in mice. *J Clin Invest* 2011;121:4138–4149
- Dwyer MA, Kazmin D, Hu P, McDonnell DP, Malek G. Research resource: nuclear receptor atlas of human retinal pigment epithelial cells: potential relevance to age-related macular degeneration. *Mol Endocrinol* 2011;25:360–372
- Zheng L, Gong B, Hatala DA, Kern TS. Retinal ischemia and reperfusion causes capillary degeneration: similarities to diabetes. *Invest Ophthalmol Vis Sci* 2007;48:361–367
- Li Calzi S, Purich DL, Chang KH, et al. Carbon monoxide and nitric oxide mediate cytoskeletal reorganization in microvascular cells via vasodilator-stimulated phosphoprotein phosphorylation: evidence for blunted responsiveness in diabetes. *Diabetes* 2008;57:2488–2494
- Segal MS, Shah R, Afzal A, et al. Nitric oxide cytoskeletal-induced alterations reverse the endothelial progenitor cell migratory defect associated with diabetes. *Diabetes* 2006;55:102–109
- Sica DA, Bakris GL. Type 2 diabetes: RENAAL and IDNT—the emergence of new treatment options. *J Clin Hypertens (Greenwich)* 2002;4:52–57
- Iwai M, Horiuchi M. Devil and angel in the renin-angiotensin system: ACE-angiotensin II-AT1 receptor axis vs. ACE2-angiotensin-(1–7)-Mas receptor axis. *Hypertens Res* 2009;32:533–536